약학석사학위논문

Discovery of anthrax biomarker candidates from human aortic endothelial cells

인간 대동맥 내피세포 모델에서의 탄저 바이오마커 후보 발굴

2014년 8월

서울대학교 대학원
약학과 병태생리학전공
조 혜 은

ABSTRACT

Discovery of anthrax biomarker candidates from human aortic endothelial cells

JOE HAE EUN
College of pharmacy
The Graduated School
Seoul National University

Anthrax, a zoonotic disease caused by *Bacillus anthracis*, is classified as cutaneous, gastrointestinal, or inhalational anthrax depending on the route of infection. The most threatening and fatal form is inhalational anthrax, which can be used as a biological weapon. *B. anthracis* releases three types of toxins, protective antigen, lethal factor, and edema factor that cause vascular and organ hemorrhage, and eventually fatal damage to the host. Since the early symptoms of inhalational anthrax are similar to those of the common cold, the status of infection is difficult to recognize. Moreover, any monitoring and prognostic tools have not been developed to predict recovery of anthrax patients. Therefore, infected patients receive late or unsuitable treatments, contributing to their increased mortality rate. Our purpose in this study was to identify the candidates of surrogate biomarker for anthrax that can be used to rapidly diagnose and monitor treatment outcomes.

To evaluate the effects of anthrax toxins–lethal toxin (LT) and edema toxin (ET)–, cytotoxicity, cell growth inhibition, and cell morphology were analyzed in primary human aortic endothelial cells (HAECs). ET induced morphological changes in HAECs while maintaining cell viability similar to that of the control group. LT reduced cell viability in a concentration- and time-dependent manner.

To discover the candidates of surrogate biomarker, secretome from anthrax toxin-treated HAECs was analyzed by using nano-liquid chromatography electrospray ionization tandem mass spectrometry. Proteins significantly upregulated or downregulated in comparison to the control group were selected, and four proteomic candidates were confirmed using immunoblot analysis. Therefore, lactotransferrin, pregnancy zone protein, and sarcolemmal membrane-associated protein were identified as proteomic candidates of anthrax biomarker.

In addition, we analyzed exosomal small RNAs and miRNAs secreted from toxin-treated HAECs by using expression array and microarray to discover transcriptomic candidates. One miRNA and several small RNAs were selected and verified using real-time quantitative reverse transcription polymerase chain reaction. As a results, *ASPH, CD151, HSP90AA1, ICAM2, LYPD1, MPST, NUAK1* and *hsa-miR-1307-3p* were found as transcriptomic candidates of anthrax biomarker. We intend to confirm the clinical utility of these proteomic and transcriptomic candidates as anthrax biomarker using sera obtained from rat injected with anthrax toxins.

In this study, three proteins, seven small RNAs, and one miRNA were identified and validated in an *in vitro* anthrax model. These results suggested that

secretory proteins and exosomal RNAs could be used as putative anthrax biomarkers for early diagnosis and treatment monitoring.

Keywords : Anthrax, Anthrax toxins, HAECs, Secretome, Exosomal RNA, Biomarker

Student number **:** 2012-23602

CONTENTS

LIST OF FIGURES

LIST OF TABLES

LIST OF ABBREBIATIONS

PA	Protective antigen
LF	Lethal factor
EF	Edema factor
LT	Lethal toxin
ET	Edema toxin
cAMP	Cyclic adenosine monophosphate
ELISA	Enzyme-linked immunosorbent Assay
Ig	Immunoglobulin
HAECs	Human aortic endothelial cells
AFP	Alpha-fetoprotein
LTF	Lactotransferrin
PZP	Pregnancy zone protein
SLMAP	Sarcolemmal-membrane associated protein
miRNA	Micro-ribonucleic acid
cRNA	Complementary ribonucleic acid
rRNA	Ribosomal ribonucleic acid
qRT-PCR	Real-time quantitative reverse transcription polymerase chain reaction
cDNA	Complementary deoxyribonucleic acid
ASPH	Aspartate beta-hydroxylase
CD151	CD151 molecule (Raph blood group)

HSP90AA1	Heat shock protein 90kDa alpha (cytosolic), class A member 1
ICAM2	Intercellular adhesion molecule 2
LYPD1	LY6/PLAUR domain containing 1
MPST	Mercaptopyruvate sulfurtransferase
NUAK1	NUAK family, SNF1-like kinase, 1
ARHGDIA	Rho GDP dissociation inhibitor (GDI) alpha (ARHGDIA), transcript variant 2
PGK1	Phosphoglycerate kinase 1 (PGK1)
PPP1R10	Protein phosphatase 1, regulatory subunit 10 (PPP1R10), transcript variant 1
RPS27A	Ribosomal protein S27a, transcript variant 1

INTRODUCTION

Anthrax is an infectious disease caused by *Bacillus anthracis*, a gram-positive, aerobic, and rod-shaped bacterium [1]. *B. anthracis* releases three types of toxins: protective antigen (PA), lethal factor (LF), and edema factor (EF) [1-3]. PA combines LF or EF to form lethal toxin (LT) or edema toxin (ET) respectively, the major virulence factors of anthrax. PA plays a key role in binding to anthrax receptors (tumor endothelial marker 8 and capillary morphogenesis protein 2) and translocating LF or EF into the cytoplasm of infected cells. LF is capable of inducing apoptosis by cleaving mitogen-activated protein kinases. In contrast to LF, EF causes edema by inducing an increase in intracellular cAMP, disrupting water homeostasis in infected cells [2, 3].

Anthrax is caused by the entry of *B. anthracis* spores through the skin (cutaneous anthrax), gastrointestinal mucosa (gastrointestinal anthrax), or the lungs (inhalational anthrax) [1]. The spores can be produced *in vitro* with ease and can lead to large numbers of casualties even in small quantities. For that reason, anthrax spores are among the most threatening agents used as a biological weapon [4-8].

Anthrax symptoms depend on the type of infection. For cutaneous anthrax, symptoms include an immediate appearance of small blisters or bumps that form black centers [6, 7]. As for gastrointestinal anthrax, symptoms are severe abdominal pain, blood vomit, and bloody diarrhea. While the symptoms of cutaneous and gastrointestinal anthrax are clearly visible, early symptoms of inhalational anthrax are not as distinctive since they are similar to those of the common cold such as sore throat and mild fever [7, 9]. Thus, cases of inhalational

anthrax are difficult to recognize before appearance of serious symptoms such as bleeding. The emergence of late symptoms enables anthrax diagnosis; however, by that time, the bacteria and toxins may have already spread to the blood. Thus, a patient's chance of recovery is limited despite the use of clinical therapies such as antibiotics. The ability to differentially diagnose anthrax and cold-like illnesses is challenging and tools for monitoring anthrax are required to determine the appropriate types and doses of medicine for each patient. Although many researchers are striving to solve these problems, no optimally therapeutic, diagnostic, and prognostic tools have been developed to date.

Hematological tests are non-invasive, sensitive, and specific tools that have been used to detect therapeutic biomarkers for various diseases. In patients with presumptive *B. anthracis* infection, the bacteria are identified by specimen tests and Gram staining [9, 10]. Unfortunately, these tests can only determine the presence or absence of *B. anthracis*, but not the status of infection. Enzyme-linked immunosorbent assay is also a valuable and sensitive method to detect immunoglobulin G induced by *B. anthracis* [9]. In some patients, however, PA-specific IgG antibody detection could occur too late, because these antibodies are detectable between 10 and 40 days after the onset of symptoms [9]. As the prognosis of anthrax patients depends on the exposure time of *B. anthracis*, an exact diagnosis should be made as soon as possible for proper treatment and monitoring of the patient's condition. Therefore, the need for early diagnosis and new therapies is on the rise. Identification of more useful and significant surrogate biomarkers will be helpful in recognizing anthrax.

Although macrophages have been used as an *in vitro* model in several

previous anthrax studies [11, 12], endothelial cells have more advantages [13, 14]. The results of both clinical and experimental studies suggest that blood vessels are the primary target tissue for anthrax pathogenesis [13, 15]. Bleeding, including hemorrhagic mediastinitis, lymphadenitis, and tissue hemorrhage, is a major factor leading to anthrax-associated death. In addition, human aortic endothelial cells (HAECs) express high levels of anthrax toxin receptors compared to macrophages [14]. By targeting HAECs, anthrax toxins contribute to vascular damage.

The study of molecules reflecting anthrax status is useful in the discovery of potential biomarkers. As both secretome and exosome reflect various states of cells under normal and pathological conditions, they can serve as sources of significant biomarkers [16-20]. Secretome, the set of proteins secreted by various cells, plays an essential part in cell-to-cell signaling and communication [16, 18]. Similar to secretome, exosome, 30 to 120 nm-sized vesicles containing proteins and RNAs (small RNAs, miRNAs, and non-coding RNAs), is released into the body fluids by various cells to regulate physiological functions [17, 19, 20].

In this study, we hypothesized that blood composition may be changed by secretory molecules released from endothelial cells that have been affected by anthrax toxins. We also suggest that the secretory molecules induced by anthrax toxins can serve as potential biomarkers since they reflect anthrax status in real time.

Therefore, in this study, we aimed to identify surrogate biomarker candidates by analyzing the secretome and exosomal RNAs from anthrax toxin-treated HAECs. Furthermore, we expected that these experimental outcomes can be used to predict the results of hematological tests for diagnosis and prognosis.

Materials and Methods

Cell culture

Primary HAECs were purchased from Invitrogen (Carlsbad CA, USA). Cells were maintained in endothelial cell basal medium-2 (Lonza, Basel, Switzerland) supplemented with rhEGF, rhFGF-B, GA-1000, R3-IGF-1, ascorbic acid, VEGF, heparin, hydrocortisone, and 2% fetal bovine serum (FBS). Cells were grown in 100-mm dishes coated with 0.1% gelatin in phosphate-buffered saline to facilitate stable cell attachment. HAECs were detached by using Accutase (Innovative Cell Tech, San Diego, CA, USA).

Anthrax Toxins

Anthrax toxins were obtained from the Agency for Defense Development, Korea. The toxins were purified from bacterial strains carrying their encoding recombinant DNA. The concentration of purified PA, LF, and EF were 1.7, 1.8, and 1.6 mg/mL, respectively.

Cell viability assays and real-time live cell imaging

Cells were seeded at a density of 8000 cells per well in 96-well plates and treated with 0.01, 0.1, 1, 10, 100, and 1000 ng/mL of LT or ET in presence 500 ng/mL of PA. Cells were incubated for 12, 24, 36, and 72 h at 37℃ in a humidified atmosphere containing 5% CO_2, and were imaged using the IncuCyte ZOOM

(Essen BioScience, Inc., Ann Arbor, MI, USA). Cell viability was measured using a water-soluble tetrazolium (WST) colorimetric assay (Ez-Cytox, Daeil Lab Service, Seoul, Korea). Absorbance was measured at 450 nm by using a SpectraMax M5 microplate reader (Molecular Devices, Sunnyvale, CA, USA). Cells in the negative control group were cultured in complete medium with only 500 ng/mL of PA or without toxins.

Concentration and quantification of secretome

Cells were seeded in 100-mm dishes. When cells reached 100% confluency, they were treated with 1000 ng/mL of LF or EF in the presence of 500 ng/ml PA dissolved in serum-free supplemented medium. LT-treated cells were incubated for 12 and 18 h and ET-treated cells were incubated for 4 and 8 h. Cells in the negative control group were cultured for 12 h in medium without FBS. At each time point after toxin treatment, cell culture supernatants were collected and centrifuged at 230 × g for 10 min at 4℃ to remove cells and debris. The supernatants were transferred to Amicon Ultra Centrifugal 3K filter tubes (Millipore, Billerica, MA, USA) and concentrated 200-fold at 5,000 × g. Total protein concentrations of the samples were determined using colorimetric Bradford reagent (BioRad, Hercules, CA, USA) and Biophotometer (Eppendorf, Hamburg, Germany). Bovine serum albumin and distilled water were used as the standards and blank, respectively. Concentrated samples were used for nano-LC-ESI-MS/MS and immunoblot analysis.

Sodium dodecyl sulfate polyacrylamide gel electrophoresis

Proteins in the concentrated supernatants were quantified using a microBCA™ protein assay kit (Pierce, Rockford, IL, USA). Equal amounts of protein (50 μg) were then separated on NuPAGE® 4–12% Bis-Tris gels (Invitrogen). After separation, the gels were stained using GelCode® Blue Stain Reagent (Thermo Scientific Inc., Rockford, IL, USA). The blue-stained gel lanes were removed by manual cutting and then sliced into five pieces. Each of the gel slices were further cut into sizes of ~1 mm^3 and transferred to clean 1.5-mL tubes.

In-gel tryptic digestion

The proteins separated by sodium dodecyl sulfate polyacrylamide gel electrophoresis (SDS-PAGE) were excised from the gel. The protein-containing gel pieces were destained using 50% acetonitrile (ACN) with 50 mM NH_4HCO_3 and vortexed until coomassie brilliant blue was completely removed. The gel pieces were then dehydrated in 100% ACN and vacuum-dried for 20 min in a SpeedVac (Labconco Corporation, Kansas City, MO, USA). For digestion, the gel pieces were reduced using 10 mM dithiothreitol in 50 mM NH_4HCO_3 for 45 min at 56℃, followed by alkylation by using 55 mM iodoacetamide in 50 mM NH_4HCO_3 for 30 min in the dark. Finally, each gel pieces was treated with 12.5 ng/μL sequencing-grade modified trypsin (Promega, Madison, WI, USA) in 50 mM NH_4HCO_3 buffer (pH 7.8) at 37℃ overnight. Following digestion, tryptic peptides were extracted using 5% formic acid in 50% ACN solution at room temperature for 20 min. The supernatants were collected and dried by SpeedVac

(Labconco Corporation). The samples were purified and concentrated in 0.1% formic acid by using C18 ZipTips (Millipore) prior to MS analysis.

Nano-liquid chromatography electrospray ionization tandem mass spectrometry

The tryptic peptides were loaded onto a fused silica microcapillary column (12 cm × 75 µm) packed with C18 reversed-phase resin (5 µm, 200 Å). LC separation was performed under a linear gradient as follows: 3–40% solvent B (0.1% formic acid in 100% ACN) gradient, with a flow rate of 250 nL/min for 60 min. The column was directly connected to Thermo's Finnigan LTQ linear ion-trap mass spectrometer (Thermo Electron Corporation, San Jose, CA, USA) equipped with a nano-electrospray ion source. The electrospray voltage was set at 1.95 kV, and the threshold for switching from MS to MS/MS was 500. The normalized collision energy for MS/MS was 35% of the main radio frequency amplitude and the duration of activation was 30 ms. All spectra were acquired in data-dependent scan mode. Each full MS scan was followed by five MS/MS scans corresponding from the most intense to the fifth most intense peaks of the full MS scan. The repeat count of the peak for dynamic exclusion was 1, and its repeat duration was 30 s. The dynamic exclusion duration was set for 180 s and width of exclusion mass was ± 1.5 Da. The list size of dynamic exclusion was 50.

Database search and proteomics validation

The acquired nano-LC-ESI-MS/MS fragment spectra were searched, using the BioWorksBrowser™ (version Rev. 3.3.1 SP1, Thermo Fisher Scientific Inc.) with the SEQUEST search engines, against the National Center for Biotechnology Information (http://www.ncbi.nlm.nih.gov/) non-redundant human database (version: Dec 17, 2012; 35720 proteins). The search conditions were trypsin enzyme specificity, permissible level for two missed cleavages, and peptide tolerance; ± 2 amu, mass error of ±1 amu on fragment ions, and fixed modifications of cysteine carbamidomethylation (+57 Da) and oxidation of methionine (+16 Da) residues. The delta CN was 0.1; the Xcorr values were 1.8 (+1 charge state), 2.3 (+2), and 3.5 (+3); and the consensus score was 10.15 for the SEQUEST criteria. Detected proteins were analyzed using the PANTHER Classification System database (http://www.pantherdb.org) for gene ontology (GO) analysis. We analyzed the samples in triplicate and selected proteins that were identified in at least two replicate analyses.

Immunoblot analysis

As described above, secreted proteins were concentrated and quantified.

Cells were lysed using RIPA buffer (50 mM Tris pH 8.0, 150 mM NaCl, 1% Triton X-100, 0.5% sodium deoxycholate and 0.1% SDS) containing protease and phosphatase inhibitors cocktail (Roche Diagnostics, Basel, Switzerland). The protein concentrations of the samples were measured using a BCA protein assay reagent kit (Thermo Scientific Inc.). Both secretory and cellular proteins were

resolved using 8% SDS-PAGE and transferred to 0.2-μm polyvinylidene fluoride membranes (Millipore). The membranes were blocked in 5% non-fat milk in 0.1% Tris-buffered saline containing Tween-20 (TBS-T) for 1 h. The blots were then incubated with primary antibodies diluted 1:2,000 in 1% non-fat milk dissolved in TBS-T on a shaker overnight at 4℃. The primary antibodies used were as follows: α-fetoprotein (AFP; C3, sc-8399, Santa Cruz Biotechnology, Dallas, TX, USA), pregnancy zone protein (PZP; 21742-1-AP, Proteintech, Chicago, IL, USA), lactotransferrin (LTF; KT33, sc-101487, Santa Cruz Biotechnology), sarcolemmal membrane-associated protein (SLMAP; A01, H00007871-A01, Abnova, Taipei, Taiwan). Blots were washed three times for 10 min each with TBS-T and incubated with HRP-conjugated goat anti-mouse or goat anti-rabbit secondary antibodies diluted 1:10,000 and 1:20,000 in TBS-T containing 1% non-fat milk on a shaker for 2 h at room temperature. The β-actin antibody (C4, sc-47778, Santa Cruz Biotechnology) was used as a quantifiable loading control. Protein bands were detected using ECL solution (GE Healthcare, Buckinghamshire, UK).

Exosomal RNA isolation

Cells were seeded in 100-mm dishes and treated with 1000 ng/mL of LF or EF in the presence of 500 ng/mL PA dissolved in serum-free supplemented medium. The LT- and ET-treated groups were incubated for 4, 6, and 12 h. Cells in the negative control groups were cultured for 12 h in medium without FBS. At each time point after toxin treatment, cell culture supernatants were collected and centrifuged at 3,000 × g for 15 min at 4℃ to remove cells and debris. The supernatants were

transferred to new tubes and mixed with ExoQuick-TC Exosome precipitation solution (System Biosciences, CA, USA) for 24–48 h at 4℃, following a modified version of the manufacturer's protocol. Exosomal RNAs were isolated using Hybrid-R miRNA kit (GeneAll Biotechnology, Seoul, Korea) according to manufacturer's instructions. After isolation of the exosomal RNAs, DNA contamination was removed by DNase I and samples were cleaned using Riboclear™ plus (GeneAll Biotechnology).

RNA quality control

The concentrations of exosomal RNAs were measured using a Qubit Fluorometer (Invitrogen). The purities of the exosomal RNAs were determined using a NanoDrop spectrophotometer (Thermo Fisher Scientific). The ratio of absorbance at 260/280 nm was between 1.8 and 2.1 and the ratio of absorbance at 260/230 nm was greater than 1.5 for each sample. The assessment of exosomal RNA quality was performed using an Agilent 2100 Bioanalyzer (Agilent Technologies, Santa Clara, CA, USA).

Small RNA expression array

Small RNA expression profiling analysis was performed using an Agilent human gene expression 4 × 44 K v2 Microarray kit (Agilent Technologies). Labeling and hybridization were performed following the manufacturer's instructions. Briefly, 100 ng of exosomal RNAs was amplified and labeled with Cyanine 3-CTR (Cy3) using Agilent's One-color Low Input Quick Amp Labeling Kit, following the

instructions provided. Next, 1650 ng of Cy3-labeled complementary RNA (cRNA) was hybridized to 4 × 44 K Microarray Chips (Agilent Technologies) for 17 h at 65℃ according to the manufacturer's recommendations. Fluorescence signals of the hybridized Agilent Microarrays were detected using Agilent Microarray Scanner C. After washing and scanning, the signals were analyzed using the GeneSpring GX analysis software version 12.6 (Agilent Technologies). Exosomal small RNAs were analyzed using PANTHER Classification System database (http://www.pantherdb.org) for GO analysis.

MicroRNA microarray

For miRNA microarray, 100 ng of exosomal RNAs was labeled with Cy3-pCp molecule and hybridized to a Human miRNA Microarray Release 14.0, 8 × 15 K Chip (Agilent Technologies) for 20 h at 55℃ according to the manufacturer’s instructions. After washing the hybridized microarray chip, fluorescent signals were measured using Agilent Microarray Scanner C (Agilent Technologies) and analyzed using the GeneSpring GX analysis software version 12.6 (Agilent Technologies). MicroRNA target genes were analyzed using DIANA-microT-CDS (http://www.microrna.gr/microT-CDS), miRNA target prediction software (http://www.isical.ac.in/~bioinfo_miu/targetminer20.htm), TargetScanHuman 6.2 (http://www.targetscan.org/), miRDB (http://mirdb.org/miRDB/mining.html), and RNA22 version 1.0 tool (https://cm.jefferson.edu/rna22v1.0/). Predicted target genes were analyzed using the PANTHER Classification System database for gene ontology (GO) analysis.

Real-time quantitative reverse transcription polymerase chain reaction

To verify the exosomal small RNA microarray data, real-time quantitative reverse transcription polymerase chain reaction (qRT-PCR) was performed. In briefly, 2 μg of exosomal small RNAs was used to generate cDNA using the Transcriptor First-Strand cDNA Synthesis Kit (Roche Applied Science, Mannheim, Germany) according to manufacturer's instructions. To verify the exosomal miRNA microarray data, 6.67 ng of exosomal RNAs including miRNAs was used to generate cDNA using the TaqMan® MicroRNA reverse Transcription Kit (Applied Biosystems, Foster City, CA, USA). After both cDNAs were diluted from two- to eight-fold, qPCR was performed using a LightCycler® 480 System (Roche Applied Science). *ASPH, CD151, HSP90AA1, ICAM2, LYPD1, MPST,* and *NUAK1* primers were designed to recognize common regions of these genes by using ProbeFinder Software v2.50 (http://www.roche-applied-science.com, Roche Applied Science) and IDT PrimerQuest (www.idtdna.com/Primerquest, Integrated DNA Technologies, Coralville, IA, USA). *hsa-miR-1307-3p* primers were designed using the Custom TaqMan® Small RNA Assay Design Tool (Life Technologies, Carlsbad, CA, USA) and synthesized by Cosmogenetech (Seoul, Korea). Commercial Universal Probe Library (UPL) probes were purchased from Roche Applied Science. *ARHGDIA, PGK1, PPP1R10,* and *RPS27A* were used as small RNA reference genes, whereas *RNU6B, RNU48,* and *hsa-miR-320a* were used as miRNA reference gene in qRT-PCR for normalization of the expression levels (ΔΔCt method).

RESULTS

Anthrax toxins induced human aortic endothelial cell death or morphological changes.

To examine the effects of anthrax toxins (LT and ET) on HAECs, cytotoxicity was determined by using a WST assay while cell growth inhibition and morphology were observed using a real-time live cell-imaging instrument. Cells were treated with 0.01, 0.1, 1, 10, 100, 1000 ng/mL LF or EF in the presence of 500 ng/mL PA. As shown in Figure 1A and B, LT induced concentration- and time-dependent reductions in cell viability and growth. In the LT-treated groups, cell death increased at 48 h when at least 1 ng/mL LT (500 ng/mL PA + 1 ng/mL LF) was administered (Fig. 2).

In contrast to LT treatment, ET treatment did not have as a significant effect as LT on cells when compared to the control group (Fig. 3A and B). In ET treatment groups, cells adopted rounded morphologies and lost viability at 72 h after treatment (Fig. 4).

Identification of proteomic biomarker candidates by using nano liquid chromatography electrospray ionization tandem mass spectrometry.

The secretome from concentrated supernatants was separated using SDS-PAGE, followed by visualization with Coomassie brilliant Blue-staining (Fig. 5). Compared to the negative control lane, toxin-treated group lanes had markedly different banding patterns. Separated proteins were digested by trypsin and identified using nano-LC-ESI-MS/MS. Identified proteins were searched against bioinformatics databases as described in the Materials and Methods, and yielded 245 and 225 proteins for the LT- and ET-treated groups, respectively. To select significant candidates, the proteins were classified as having > 2-fold higher and < 0.5-fold lower levels compared to those in the control. Based on these criteria, 44 proteins upregulated and 43 downregulated proteins in LT-treated group, whereas 29 upregulated and 43 downregulated proteins in the ET-treated group were selected.

To distinguish potential primary candidates, we selected the proteins that were upregulated or downregulated in every experimental group. Seven upregulated proteins (α-2-HS-glycoprotien, α-2-macroglobulin, AFP, inter-α-trypsin inhibitor heavy chain H2, LTF isoform 2, PZP, and SLMAP) and four downregulated proteins (78 kDa glucose-regulated protein, cadherin-5, hedgehog-interacting protein, and proactivator polypeptide isoform b) were selected for further evaluation.

LTF, PZP, and SLMAP were confirmed as surrogate anthrax biomarkers by using immunoblot analysis.

The seven upregulated proteins and four downregulated proteins were confirmed using immunoblot analysis. First, the candidates were sorted based on their absence or low presence in normal plasma. Thus, AFP, LTF, PZP, and SLMAP remained in upregulated protein group, and the four downregulated proteins (78 kDa glucose-regulated protein, cadherin-5, hedgehog-interacting protein, proactivator polypeptide isoform b) remained in downregulated protein group. Next, these eight proteins were further sorted based on their detectability in infected blood. We judged that upregulated proteins are more significant than downregulated proteins as biomarker candidates. Protein levels in the blood can vary depending on the individual patient and his/her condition. Therefore, the use of downregulated protein levels as the primary evidence for disease diagnosis is limited. Finally, four proteins−AFP, LTF, PZP, and SLMAP−were selected for further analysis as shown in Table 1.

To confirm these candidates, secreted and cellular proteins were detected by using immunoblot analysis. As shown in Figure 5A, no difference in cellular LTF was observed between the control and the treated groups. However, secreted glycosylated LTF (~90 kDa) was observed solely in the treated groups. In the secretome, PZP was cleaved to different sized fragments in each group. Under all treatment conditions, cellular PZP was detected in all groups (Fig. 5B). As shown in Figure 5C, secreted SLMAP but no cellular SLMAP was observed in the LT-

treated groups. AFP is highly abundant in human fetal plasma, but begins to decrease after birth to concentration below 5 ng/mL. AFP is used as a clinical marker, as its levels are elevated in some disease such as hepatocellular carcinoma. However, in this study, neither secreted nor cellular AFP was found.

Plasma protein levels are constantly changing according to a patient's infection status, and thus, making the detection of medically meaningful changes more difficult. We obtained list of secretome by using nano-LC-ESI-MS/MS, and sorted the potential candidates based on their significance and detectability. Results showed that LTF, PZP and SLMAP could be putative anthrax biomarkers.

Identification of transcriptomic biomarker candidates using expression array and microarray.

To screen exosomal RNAs, quality control of the extracted exosomal RNAs was performed using the Agilent 2100 Bioanalyzer. As shown in Figure 7, exosomal RNAs such as small RNAs and miRNAs range in size between 25 and 500 nucleotides.

The exosomal small RNAs were screened by expression array and analyzed using GeneSpring GX software. Identified exosomal small RNAs were classified as having > 2-fold higher and < 0.5-fold lower levels compared to those in the control. As a result, 457 upregulated and 1712 downregulated small RNAs in the LT-treated group, and 450 upregulated and 2174 downregulated small RNAs in ET-treated group were classified. We selected the candidates that were detected in every experimental group and then considered their detectability in infected blood. Thus, 38 upregulated small RNAs were selected for further evaluation.

To verify these candidates, we deliberated whether biological functions of the miRNA candidates reflect the status of infection and then selected *ASPH, CD151, HSP90AA1, ICAM2, LYPD1, MPST,* and *NUAK1* (Table 2) for further analysis. To choose a suitable reference gene for qRT-PCR normalization, we chose RNAs that had constant levels in each experimental group and were known as housekeeping genes. Finally, *ARHGDIA, PGK1, PPP1R10,* and *RPS27A* were selected.

Through the same method of selecting small RNA candidates, one upregulated and four downregulated miRNA were identified. The one upregulated

miRNA were isolated as our putative biomarker; *hsa-miR-1307-3p* was chosen as a miRNA candidate. *RNU6B, RNU48,* and *hsa-miR-320a* were chosen for qRT-PCR normalization (Table 3). MicroRNAs, small non-coding RNA molecules, play a major role in regulating translation of target mRNAs through 3′ untranslated regions [21]. However, the biological function of *hsa-miRNA-1307-3p* detected in this study is unknown.

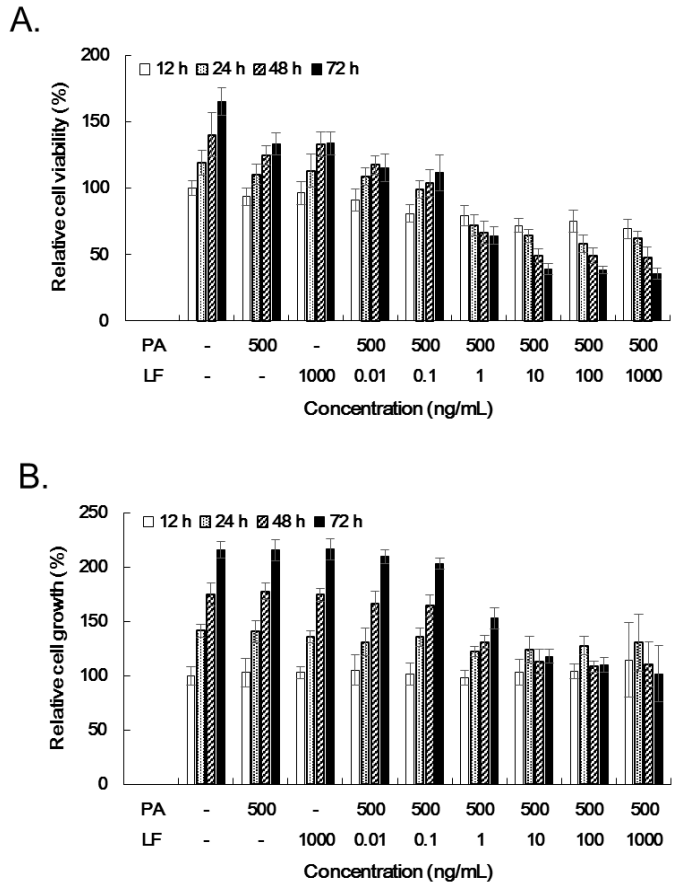

Figure 1. Concentration- and time-dependent effects of lethal toxin on human aortic endothelial cell viability and growth.

Human aortic endothelial cells (HAECs) were incubated with medium alone or medium containing 500 ng/mL protective antigen (PA), 1000 ng/mL lethal factor (LF), or various concentration of LF in presence of PA (0.01–1000 ng/mL lethal toxin [LT]) during 72 h. (A) Cell viability was measured using water-soluble tetrazolium (WST) assay. The viability of cells incubated with medium alone for 12h was used as the control. (B) Groups treated with 10–1000 ng/mL LT showed decreased cell growth. The confluence (%) of cells incubated with medium alone for 12 h was used as the control.

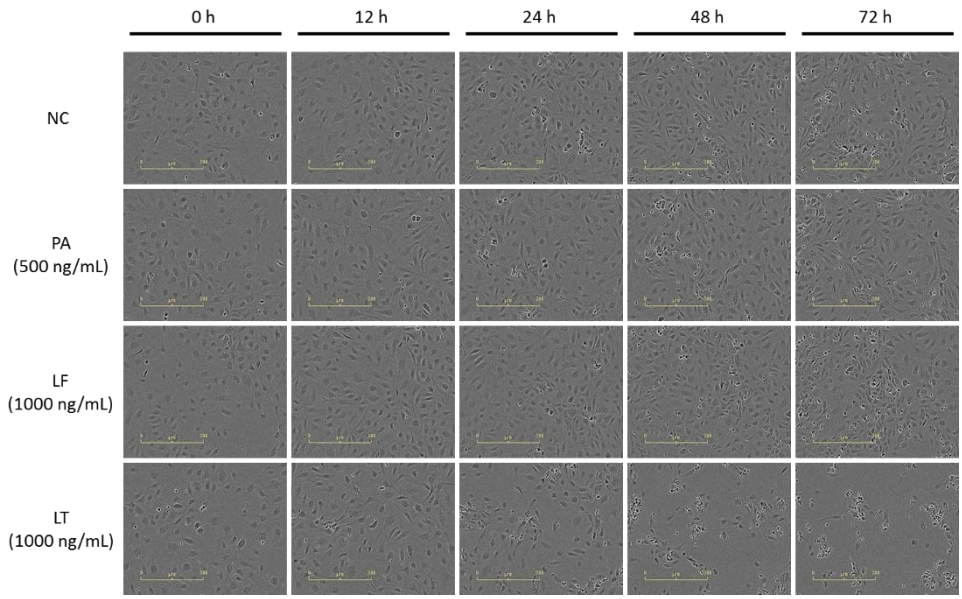

Figure 2. Lethal toxin-induced human aortic endothelial cell death.

Phase-contrast images of HAEC morphology were taken during 72 h of treatment with PA alone (500 ng/mL), LF alone (1000 ng/mL), or LT (1000 ng/mL) treatment. Negative control (NC) cells were incubated with medium alone. LT decreased cell growth and increased cell death compared to cells incubated in medium, LF or PA alone.

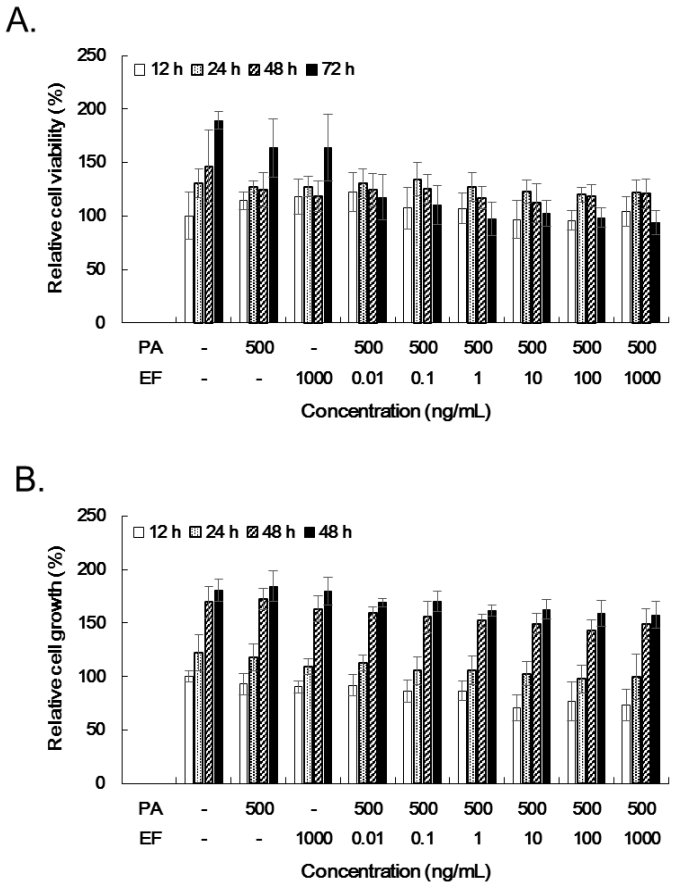

Figure 3. No effect of edema toxin on human aortic endothelial cell proliferation.

HAECs were incubated with medium alone, medium containing 500 ng/mL PA, 1000 ng/mL edema factor (EF), or various concentration of EF in the presence of PA (0.01–1000 ng/mL edema toxin [ET]) during 72 h. (A) Cell viability was measured using a WST assay. The viability of cells incubated with medium alone for 12h was used as the control. (B) ET did not inhibit cell growth until 72 h of treatment. The confluence (%) of cells incubated with medium alone for 12 h was used as the control.

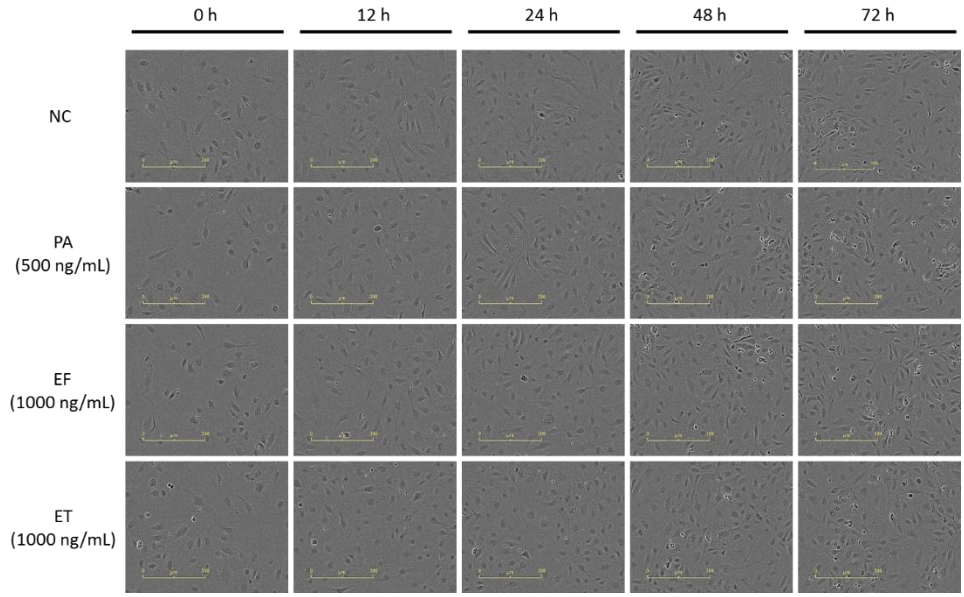

Figure 4. Edema toxin-induced morphological changes on human aortic endothelial cells.

Phase-contrast images of HAEC morphology were taken during 72 h of treatment with PA alone (500 ng/mL), EF alone (1000 ng/mL), or ET (1000 ng/mL) treatment. NC cells were incubated with medium alone. Although ET induced morphological changes, it did not affect cell growth within 72 h.

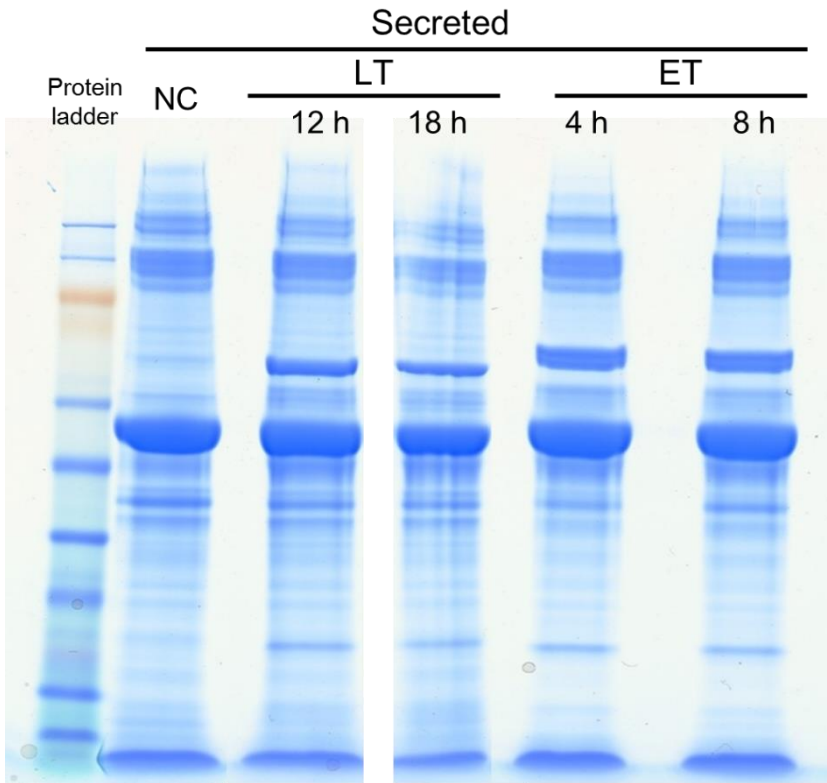

Figure 5. Sodium dodecyl sulfate polyacrylamide gel electrophoresis of the anthrax toxin-treated human aortic endothelial cell secretome.

Toxins treatments were delivered in serum-free medium containing supplementary factors. LF or EF (1000 ng/mL) was mixed with 500 ng/mL PA. NC cells were incubated with medium alone. After toxin treatment, supernatants were harvested and concentrated for nano-liquid chromatography electrospray ionization tandem mass spectrometry (nano-LC-ESI-MS/MS). Samples were then separated on 4–12% Bis-Tris gel and stained with GelCode® Blue. The difference among the samples were examined visually.

Table 1. Four proteomic biomarker candidates selected for confirmation using immunoblot analysis.

Secreted proteins	Accession No.	Fold change			
		LT		ET	
		12 h	18 h	4 h	8 h
AFP (69 kDa)	NP_001125.1	7.99	4.60	16.14	10.95
LTF isoform 2 (73 kDa)	NP_001186078.1	7.82	5.80	18.90	10.84
PZP (164 kDa)	NP_002855.2	7.32	3.38	15.44	11.97
SLMAP (93 kDa)	NP_009090.2	6.19	3.13	15.06	7.43

The acquired nano-LC-ESI-MS/MS fragment spectra were searched against database as described in the Materials and Method. Non-significant proteins were screened out and candidates identified in all of the groups were selected, resulting in seven upregulated proteins. Through final sorting of excluding abundant proteins, AFP, LTF, PZP, and SLMAP were selected for confirmation.

Abbreviations: AFP, α-fetoprotein; LTF, lactotransferrin; PZP, pregnancy zone protein; and SLMAP, sarcolemmal membrane-associated protein.

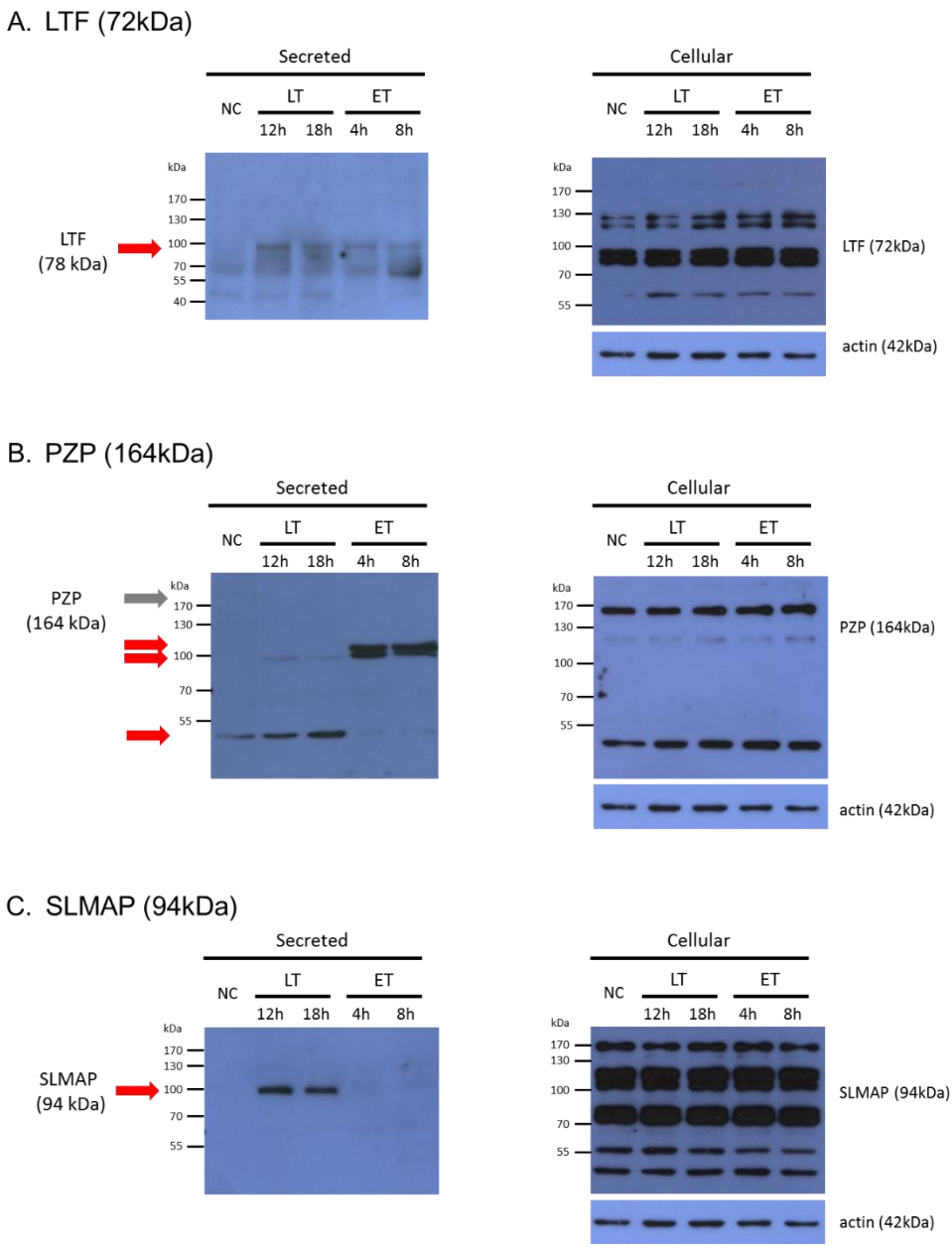

Figure 6. Secreted LTF, PZP, and SLMAP as significant candidates of anthrax biomarker.

Figure 6. Secreted LTF, PZP, and SLMAP as significant candidates of anthrax biomarker. (*Continued*)

(A, B, C) AFP, LTF, PZP, and SLMAP were confirmed using immunoblot analysis. LTF, PZP, and SLMAP showed different banding patterns in comparison to those of control. SLMAP was markedly different in LT-treated groups, while PZP showed different cleaved patterns according to the toxins treatment. In the blots of cellular proteins, no difference was observed between the groups.

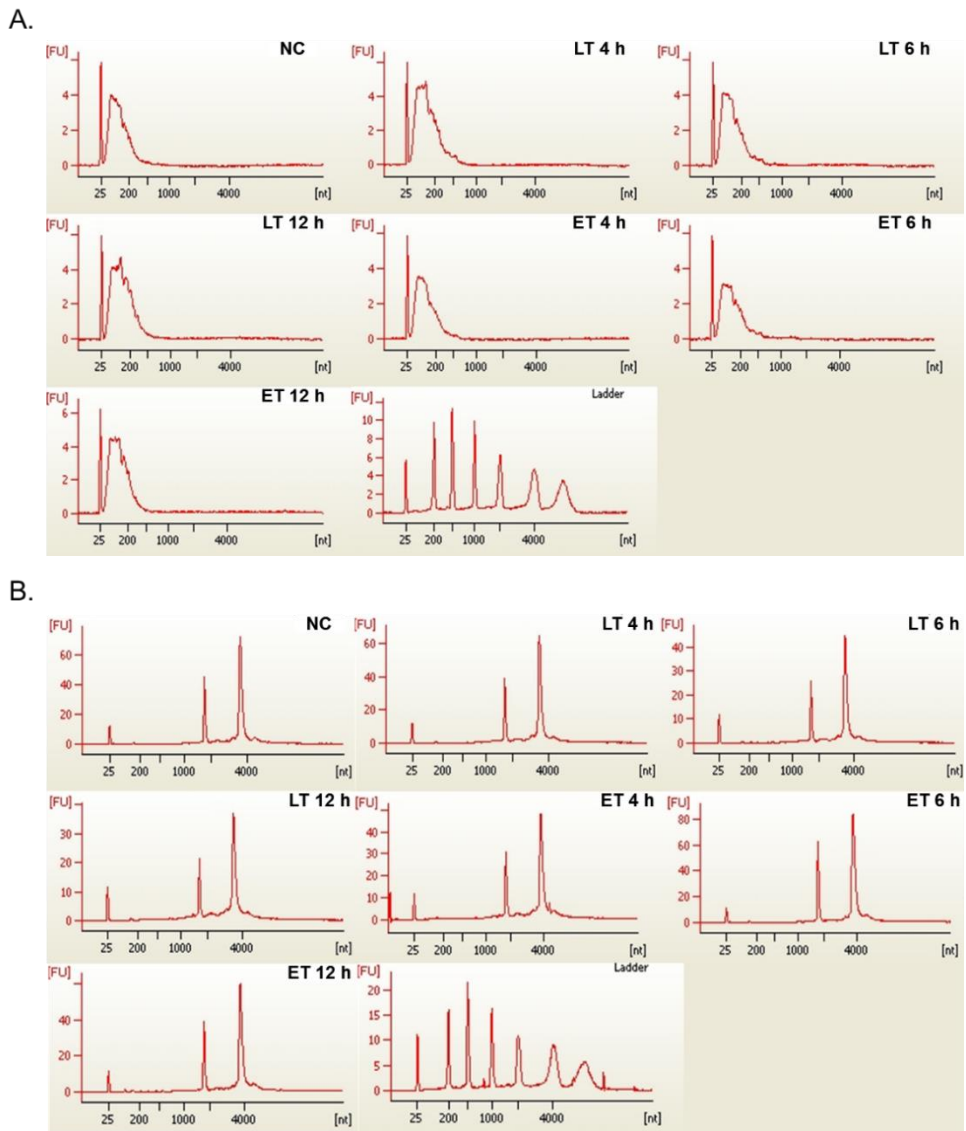

Figure 7. Small RNAs as major component of exosome secreted from human aortic endothelial cells.

The size distribution of exosomal RNAs and cellular RNAs from anthrax toxin-treated HAECs were detected using an Agilent 2100 Bioanalyzer. (A) Exosomal RNAs mostly include small RNAs less than < 200 nucleotides, (B) while 18S and 28S rRNAs were the most abundant cellular RNAs.

Table 2. Seven exosomal small RNA biomarker candidates selected for confirmation by using real-time quantitative reverse transcription polymerase chain reaction.

Gene symbol	Gene name (Accession No. / Chromosomal location)	Fold change					
		LT			ET		
		4 h	6 h	12 h	4 h	6 h	12 h
ASPH	aspartate beta-hydroxylase (NM_004318 / chr8:62460683-62438666)	3.37	2.61	2.88	2.01	3.94	2.87
CD151	CD151 molecule (Raph blood group) (NM_004357 / chr11:838770-838829)	8.46	4.57	6.41	2.86	4.43	3.61
HSP90AA1	heat shock protein 90kDa alpha (cytosolic), class A member 1 (NM_001017963 / chr14:102547454-102547395)	4.48	2.67	4.00	2.36	3.56	2.09
ICAM2	intercellular adhesion molecule 2 (NM_000873 / chr17:62080019-62079960)	7.87	5.45	5.95	2.21	5.29	3.40
LYPD1	LY6/PLAUR domain containing 1 (NM_144586 / chr2:133402490-133402431)	3.46	5.19	4.62	3.02	5.62	2.51
LYPD1	LY6/PLAUR domain containing 1 (NM_144586 / chr2:133402818-133402759)	5.37	4.97	3.93	2.83	5.70	4.40
MPST	mercaptopyruvate sulfurtransferase (NM_001130517 / chr22:37425669-37425728)	7.26	5.61	7.71	4.46	5.51	5.38
NUAK1	NUAK family, SNF1-like kinase, 1 (NM_014840 / chr12:106457605-106457546)	5.79	3.87	3.01	3.55	5.63	3.11

Exosomal small RNAs were screened using an expression array. The fluorescent signals were searched against database as described in the Materials and Method. Candidates identified in all of the groups were selected based on their significant biological function in relation to infection status such as response to stimuli, relation to the immune system and cellular communication. *ASPH, CD151, HSP90AA1, ICAM2, LYPD1, MPST,* and *NUAK1* were selected for real-time quantitative reverse transcription polymerase chain reaction (qRT-PCR) analysis.

Table 3. One exosomal miRNA biomarker candidate selected for confirmation by using real-time quantitative reverse transcription polymerase chain reaction.

Gene symbol	Sequence (miRBase Accession No.)	Fold change					
		LT			ET		
		4 h	6 h	12 h	4 h	6 h	12 h
hsa-miR-1307-3p	ACUCGGCGUGGCGUCGGUCGUG (MIMAT0005951)	29.58	42.77	54.95	41.73	53.15	59.29

Exosomal miRNAs were screened using microarray and 152 miRNAs were detected based on absolute fold change > 2. To classify miRNA candidates, we selected miRNAs that were detected in every experimental group; one upregulated and four downregulated miRNAs remained for further analysis. We selected one easily detectable biomarker, *hsa-miR-1307-3p*, which was the only upregulated miRNA candidate.

Table 4. Primers and probes used for using real-time quantitative reverse transcription polymerase chain reaction.

Gene		Sequence 5′ → 3′	Length (bp)	Tm
ASPH	F	ATGTGCCAACGAGACCAAG	19	59
	R	ACCTCGTGCTCAAAGGAGTC	20	59
CD151	F	TCACCACCACCCGAAATG	18	62
	R	CTGGGTACAGCAGTGAACAA	20	62
HSP90AA1	F	GATGACCCTACTGCTGATGATAC	23	62
	R	TCCCTCAGCCAGAGATTAGT	20	62
ICAM2	F	CAATGAATTCCAACGTCAGC	20	59
	R	ACCAAAGTGGGTTGCAGTGT	20	60
LYPD1	F	CGGCCAATGTCACAACAATC	20	62
	R	GCCAGTAAGCACAGAACAGA	20	62
MPST	F	TCTGCTTTCACCAAGAGAGTG	21	62
	R	TACTGGCAGCCAACAAGTC	19	62
NUAK1	F	TTCCTGGTCCTCTCCTTACTT	21	62
	R	CTGATTGTGCCTTGACATTTACC	23	62
ARHGDIA	F	GGGCAGCTACAGCATCAA	18	62
	R	TCAGTCCTTCCAGTCCTTCT	20	62
PGK1	F	GGTGGTGAAAGCCACTTCTA	20	62
	R	CTGACTTTATCCTCCGTGTTCC	22	62
PPP1R10	F	CCTGTCAACCACCTCTGAATC	21	62
	R	GTGAAGGAGAGAACTGGGAAAG	22	62
RPS27A	F	CTTCGTGGTGGTGCTAAGAA	20	62
	R	TTCAGGACAGCCAGCTTAAC	20	62

DISCUSSION

In the present study, we focused on host-derived proteins after *B. anthracis* infection in order to discover the candidates that could be used as new diagnostic and prognostic biomarkers. Previous studies reported that pathogen-derived biomarkers are useful as diagnostic tools because of their high specificity for pathogen [22-24]. However, it may be difficult to detect low level of pathogen-derived biomarkers at early stage of the infection [25]. Therefore, host-derived biomarkers, which are abundant and could immediately reflect the host status, may have more benefits compared to pathogen-derived biomarkers [25]. First, using HAECs as our *in vitro* model for anthrax study, we showed that LT induced death 48–72 h after LT treatment. This finding was similar to the reports of previous clinical studies that said progressive symptoms such as hemorrhage were observed three to five days after the onset of initial signs of disease [6, 13]. Unlike LT, ET induced morphological changes in HAECs without causing cell death during the 72 h treatment period. This is consistent with previous studies that reported ET induces morphological and cytoskeletal changes through increased cAMP expression [26]. Therefore, HAECs is an appropriate and significant *in vitro* model to analyze the effects of anthrax toxins.

To discover early host-derived anthrax biomarkers, we performed analysis of secretome and exosomal RNAs secreted from anthrax toxin-treated HAECs. The toxin incubation times used for the detection of secretome and exosomal RNAs were determined based on the results of the cell viability assay. In the secretome analysis,

we identified common diagnostic markers for bacterial infection [27-30]. In addition, coagulation cascade- and adhesion-related proteins were upregulated in comparison to the control. However, these common proteins were excluded from the list of potential anthrax biomarkers, because they were not specific to anthrax. For that reason, we selected proteins that were present in low levels under normal condition, but were upregulated under pathological conditions [31].

LTF, PZP, SLMAP, and AFP were thus selected as putative diagnostic and prognostic biomarkers. LTF is a glycoprotein secreted from exocrine glands and belongs to the innate immune system. The level of plasma LTF changes during pregnancy, and increases in infection, inflammation, and the pathogenesis of several disease [32]. In our study, LTF secretion from HAECs was observed as an effect of anthrax toxin (LT and ET) treatment. PZP, a pregnancy-associated plasma protein, is present at < 30 mg/L in the plasma of healthy, non-pregnant individuals. During pregnancy, the level of PZP increases, reaching approximately 1000–1400 mg/L in plasma [33, 34]. In immunoblot analysis, the PZP bands showed different cleavage patterns when treated with LT or ET. SLMAP is tail-anchored membrane protein that plays a role in myoblast fusion during myogenesis [35]. Interestingly, secreted SLMAP was only detected in the LT treatment groups, suggesting that this protein could be a LT-specific biomarker. Although AFP, which is found in high concentrations in fetuses and patients with liver disease [36], was identified by nano-LC-ESI-MS/MS, it could not be detected by immunoblot.

In the exosomal small RNA expression array, several of the detected genes were related to metabolic and cellular processes. We focused on those with biological functions related to anthrax status. As a results, we identified *CD151,*

ICAM2, *LYPD1*, and *NUAK1*, which are related to immunological processes; *CD151*, *HSP90AA1*, *MPST*, and *NUAK1*, which respond to stimuli; and *ASPH*, *CD151*, *HSP90AA1*, and *NUAK1* play roles in cellular communication. The physiological functions of these genes are still unknown, but there have been some studies that tried to elucidate the biological functions of these genes. *ASPH* encodes aspartate β-hydroxylase which could play a role in calcium homeostasis [37]. *CD151* encodes CD151 molecule (Raph blood group), a transmembrane 4 superfamily protein. *CD151* was reported to be released from various cell types and may be associated in neovascularization, morphogenesis, and cell-cell adhesion [38, 39]. *HSP90AA1* encodes heat shock protein (HSP) 90 kDa α class A member 1, and the HSP90 family plays an important role in cell survival, cytokine signaling, and immune responses [40]. *ICAM2* encodes intercellular adhesion molecule 2, which mediates cell-cell interaction during antigen-specific immune responses [41]. *MPST* encodes mercaptopyruvate sulfurtransferase which plays a role in the detoxification response to toxic substances such as H_2S gas [42]. *NUAK1* encodes NUAK family SNF1-like kinase 1, which is associated with cell adhesion and cell proliferation [43, 44]. These biological functions may be related to responses to anthrax such as detoxification, immune cell recruitment, and survival mechanisms against anthrax toxins.

Our studies also demonstrated that *hsa-miR-1307-3p* could be a miRNA biomarker of anthrax. However, the biological function of *hsa-miR-1307-3p* also has not been explored. We analyzed target genes of five miRNAs detected in every group using several database as described in Materials and Method. Selected target genes were matched up with genes identified by cellular RNA expression array and

were analyzed by GO analysis. As a results, several increased target genes of downregulated miRNAs seemed to be directly correlated to apoptosis, cellular defense mechanism, and other responses associated with anthrax infection.

In conclusion, we found that LTF, PZP, and SLMAP could be used as host-derived proteomic biomarkers of anthrax and *ASPH, CD151, MPST, NUAK1, HSP90AA1, ICAM2, LYPD1* and *hsa-miR-1307-3p* as host-derived anthrax transcriptomic biomarkers. However, these proteins should be confirmed *in vivo* in order to be applicable in clinical situations. We will continue in our efforts to confirm these candidates *in vivo* by using the sera obtained from rat injected with anthrax toxins [45].

In this study, we identified and validated three proteins, seven exosomal small RNAs, and one exosomal miRNA. Some of the candidates' biological functions are known to be involved in immune system, defense mechanism, and stimulus response that could be associated with the status of anthrax using toxin-treated HAECs. Therefore, the results of our study can be meaningful in the discovery of new diagnostic and prognostic anthrax biomarkers.

REFERENCES

1. Dixon TC, Meselson M, Guillemin H, Hanna PC. Anthrax. N Engl J Med **1999**; 341.
2. Young JA, Collier RJ. Anthrax toxin: receptor binding, internalization, pore formation, and translocation. Annual review of biochemistry **2007**; 76: 243-65.
3. Guichard A, Nizet V, Bier E. New insights into the biological effects of anthrax toxins: linking cellular to organismal responses. Microbes and infection / Institut Pasteur **2012**; 14(2): 97-118.
4. Abramova FA, Grinberg LM, Yampolskaya OV, Walker DH. Pathology of inhalational anthrax in 42 cases from the Sverdlovsk outbreak of 1979. Proceedings of the National Academy of Sciences of the United States of America **1993**; 90(6): 2291-4.
5. Pile JC, Malone JD, Eitzen EM, Friedlander AM. ANthrax as a potential biological warfare agent. Arch Intern Med **1998**; 158(5): 429-34.
6. Jernigan JA, Stephens DS, Ashford DA, et al. Bioterrorism-related inhalational anthrax: the first 10 cases reported in the United States. Emerg Infect Dis **2001**; 7(6): 933-44.
7. Fowler RA, Shafazand S. Anthrax bioterrorism: prevention, diagnosis and management strategies. J Bioterr Biodef **2011**; 2(2): 107.
8. Balali-Mood M, Moshiri M, Etemad L. Medical aspects of bio-terrorism. Toxicon : official journal of the International Society on Toxinology **2013**; 69: 131-42.
9. Bell DM, Kozarsky PE, Stephens DS. Clinical issues in the prophylaxis, diagnosis, and treatment of anthrax. Emerg Infect Dis **2002**; 8(2): 222-5.
10. Rafiq M, Worthington T, Tebbs SE, et al. Serological detection of Gram-positive bacterial infection around prostheses. The Journal of bone and joint surgery British volume **2000**; 82(8): 1156-61.
11. Guidi-Rontani C, Levy M, Ohayon H, Mock M. Fate of germinated Bacillus anthracis spores in primary murine macrophages. Molecular microbiology **2001**; 42(4): 931-8.
12. Pickering AK, Merkel TJ. Macrophages Release Tumor Necrosis Factor Alpha and Interleukin-12 in Response to Intracellular Bacillus anthracis Spores. Infect Immun **2004**; 72(5): 3069-72.
13. Kirby JE. Anthrax Lethal Toxin Induces Human Endothelial Cell Apoptosis. Infect

Immun **2003**; 72(1): 430-9.

14. Hun Seok Lee, Su Yeun Lee, Nirmal R, et al. Human Aortic Endothelial Cell is a Reliable Candidate for Studying Anthrax Toxins Compared with Macrophage cells. Int J Nanotechnol **2013**; 10(8/9): 756-70.
15. Warfel JM, Steele AD, D'Agnillo F. Anthrax lethal toxin induces endothelial barrier dysfunction. The American journal of pathology **2005**; 166(6): 1871-81.
16. Maurya P, Meleady P, Dowling P, Clynes M. Proteomic approaches for serum biomarker discovery in cancer. Anticancer research **2007**; 27(3a): 1247-55.
17. Bang C, Thum T. Exosomes: new players in cell-cell communication. The international journal of biochemistry & cell biology **2012**; 44(11): 2060-4.
18. Stastna M, Van Eyk JE. Secreted proteins as a fundamental source for biomarker discovery. Proteomics **2012**; 12(4-5): 722-35.
19. Inal JM, Kosgodage U, Azam S, Stratton D, Antwi-Baffour S, Lange S. Blood/plasma secretome and microvesicles. Biochimica et biophysica acta **2013**; 1834(11): 2317-25.
20. S ELA, Mager I, Breakefield XO, Wood MJ. Extracellular vesicles: biology and emerging therapeutic opportunities. Nature reviews Drug discovery **2013**; 12(5): 347-57.
21. Chen K, Rajewsky N. The evolution of gene regulation by transcription factors and microRNAs. Nat Rev Genet **2007**; 8(2): 93-103.
22. Kobiler D, Weiss S, Levy H, et al. Protective antigen as a correlative marker for anthrax in animal models. Infect Immun **2006**; 74(10): 5871-6.
23. Walz A, Mujer CV, Connolly JP, et al. Bacillus anthracis secretome time course under host-simulated conditions and identification of immunogenic proteins. Proteome science **2007**; 5: 11.
24. Sela-Abramovich S, Chitlaru T, Gat O, Grosfeld H, Cohen O, Shafferman A. Novel and unique diagnostic biomarkers for Bacillus anthracis infection. Applied and environmental microbiology **2009**; 75(19): 6157-67.
25. Narayanan A, Zhou W, Ross M, et al. Discovery of Infectious Disease Biomarkers in Murine Anthrax Model Using Mass Spectrometry of the Low-Molecular-Mass Serum Proteome. J Proteomics Bioinform **2009**; 02(09): 408-15.
26. Hong J, Doebele RC, Lingen MW, Quilliam LA, Tang WJ, Rosner MR. Anthrax edema toxin inhibits endothelial cell chemotaxis via Epac and Rap1. The Journal of biological chemistry **2007**; 282(27): 19781-7.

27. Fitchett D, Goodman S, Langer A. New advances in the management of acute coronary syndromes: 1. Matching treatment to risk. CMAJ : Canadian Medical Association journal = journal de l'Association medicale canadienne **2001**; 164(9): 1309-16.

28. Ley K, Laudanna C, Cybulsky MI, Nourshargh S. Getting to the site of inflammation: the leukocyte adhesion cascade updated. Nature reviews Immunology **2007**; 7(9): 678-89.

29. Dejana E, Tournier-Lasserve E, Weinstein BM. The control of vascular integrity by endothelial cell junctions: molecular basis and pathological implications. Developmental cell **2009**; 16(2): 209-21.

30. van Hinsbergh VW. Endothelium--role in regulation of coagulation and inflammation. Seminars in immunopathology **2012**; 34(1): 93-106.

31. Anderson NL. The Human Plasma Proteome: History, Character, and Diagnostic Prospects. Mol Cell Proteomics **2002**; 1(11): 845-67.

32. Adlerova L, Bartoskova A, Faldyna M. Lactoferrin: a review. Veterinarni Medicina **2008**; 53(9): 457-68.

33. Sand O, Folkersen J, Westergaard J, Sottrup-Jensen L. Characterization of human pregnancy zone protein. Comparison with human alpha 2-macroglobulin. J Biol Chem **1985**; 260(29): 15723-35.

34. Arbelaez LF, Bergmann U, Tuuttila A, Shanbhag VP, Stigbrand T. Interaction of matrix metalloproteinases-2 and -9 with pregnancy zone protein and alpha2-macroglobulin. Archives of biochemistry and biophysics **1997**; 347(1): 62-8.

35. Nader M, Westendorp B, Hawari O, et al. Tail-anchored membrane protein SLMAP is a novel regulator of cardiac function at the sarcoplasmic reticulum. American journal of physiology Heart and circulatory physiology **2012**; 302(5): H1138-45.

36. Soltani K. Alpha-fetoprotein: a review. J Invest Dermatol **1979**; 72(5).

37. Treves S, Franzini-Armstrong C, Moccagatta L, et al. Junctate is a key element in calcium entry induced by activation of InsP3 receptors and/or calcium store depletion. The Journal of cell biology **2004**; 166(4): 537-48.

38. Zhang XA, Kazarov AR, Yang X, Bontrager AL, Stipp CS, Hemler ME. Function of the tetraspanin CD151-alpha6beta1 integrin complex during cellular morphogenesis. Molecular biology of the cell **2002**; 13(1): 1-11.

39. Zheng Z, Liu Z. CD151 gene delivery activates PI3K/Akt pathway and promotes neovascularization after myocardial infarction in rats. Molecular medicine **2006**;

12(9-10): 214-20.

40. Kakeda M, Arock M, Schlapbach C, Yawalkar N. Increased expression of heat shock protein 90 in keratinocytes and mast cells in patients with psoriasis. Journal of the American Academy of Dermatology **2014**; 70(4): 683-90 e1.

41. Rojtinnakorn J. ICAM-2, A Protein of Antitumor Immune Response in Mekong Giant Catfish (Pangasianodon gigas). International Journal of Biological, Veterinary, Agricultural and Food Engineering **2014**; 8(4): 1-5.

42. Bhatia M. Role of hydrogen sulfide in the pathology of inflammation. Scientifica **2012**; 2012: 159680.

43. Ye X-t, Guo A-j, Yin P-f, Cao X-d, Chang J-c. Overexpression of NUAK1 is associated with disease-free survival and overall survival in patients with gastric cancer. Med Oncol **2014**; 31(7): 1-8.

44. Hou X, Liu JE, Liu W, Liu CY, Liu ZY, Sun ZY. A new role of NUAK1: directly phosphorylating p53 and regulating cell proliferation. Oncogene **2011**; 30(26): 2933-42.

45. Migone T-S, Subramanian GM, Zhong J, et al. Raxibacumab for the Treatment of Inhalational Anthrax. N England J M **2009**; 361(2): 135-44.

국 문 초 록

탄저병(Anthrax)은 탄저균(Bacillus anthracis) 감염에 의해 발생하는 인수공통전염병으로 감염경로에 따라 피부탄저, 장탄저, 폐탄저로 분류된다. 탄저균은 세 가지 독소(Protective antigen, Lethal factor, Edema factor)를 분비하며, 분비된 독소들은 순환계를 통해 전신으로 운반되어 각종 장기 및 혈관에서 출혈을 야기하고 숙주에게 치명적인 손상을 일으킨다. 특히 생물 무기로 악용될 수 있는 폐탄저의 경우 초기 증상이 감기와 유사하기 때문에 치료 시기를 놓칠 경우 치사율이 급격히 증가하게 된다. 따라서, 본 연구에서는 탄저균 감염을 빠르게 진단하고 탄저병 치료의 예후를 모니터링 할 수 있는 생물학적 표지인자(Biomarker)에 대한 연구를 수행하였다.

본 연구의 모델시스템인 인간 대동맥 내피세포(Primary human aortic endothelial cells, HAECs)에서 탄저 독소의 영향을 보기 위하여 cytotoxicity, cell growth inhibition 및 cell morphology를 관찰하였다. 그 결과 치사독소(Lethal toxin, LT)를 처리한 군이 대조군에 비해 농도 의존적으로 cell viability가 감소하는 것을 관찰할 수 있었으며, 이와는 대조적으로 부종독소(Edema toxin, ET)를 처리한 군에서는 세포의 morphology만 변할 뿐 cell viability는 대조군과 유사하게 유지되는 것을 확인할 수 있었다.

본 연구의 목적인 탄저병 biomarker 후보를 탐색하기 위하여 탄저 독소 LT와 ET에 의해 HAECs이 분비하는 단백질(Secretome)을 분리하여 nano-LC-ESI-MS/MS 기법으로 동정하였다. 그리고 후보단백질을 immunoblot 기법으로 verification하였으며, 그 결과 Lactotransferrin (LTF), Pregnancy zone protein (PZP), 그리고 Sarcolemmal membrane-associated protein (SLMAP)이 탄저병 biomarker 후보단백질로의 가능성이 있음을 확인하였다.

또한 탄저 독소 LT와 ET에 의해 HAECs에서 유리된 exosomal small RNA와 miRNA를 추출하여 각각 Expression array와 Microarray 기법을 통해 또 다른 탄저병 biomarker 후보를 동정하였다. 그 결과 exosomal small RNA 후보로는 *ASPH, CD151, HSP90AA1, ICAM2, LYPD1, MPST,* 그리고 *NUAK1*를 찾아내었고, exosomal miRNA 후보로는 *hsa-miR-1307-3p*를 찾아내었다. 그리고 후보 exosomal RNA를 qRT-PCR 기법을

통해 verification하였다. 더 나아가 탄저 독소를 주입한 rat으로부터 얻은 serum에서 본 연구에서 동정한 후보 biomarker에 대한 verification을 수행하여 clinical utility를 확인할 계획이다.

따라서, 본 연구에서는 탄저병의 세포배양 모델에서 탐색한 host-derived biomarker로서 단백질 3 종, mRNA 7 종, 그리고 miRNA 1 종을 동정 및 validation 하였으며, 이러한 11종의 proteomic 및 transcriptomic biomarkers가 탄저병의 진단과 치료 효과 모니터링에 사용될 가능성을 제시하였다.

주요어 : 탄저병, 탄저독소, HAECs, Secretome, Exosomal RNA, Biomarker
학번 : 2012-23602